Forest Ecology and Management 548 (2023) 121406

Contents lists available at ScienceDirect

Forest Ecology and Management

journal homepage: www.elsevier.com/locate/foreco

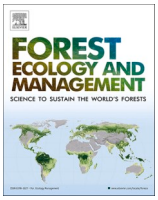

Radial growth, wood anatomical traits and remote sensing indexes reflect different impacts of drought on Mediterranean forests

Santain S.P. Italiano [a], J. Julio Camarero [b], Marco Borghetti [a], Michele Colangelo [a,b], Manuel Pizarro [b], Francesco Ripullone [a,*]

[a] Scuola di Scienze Agrarie, Forestali, Alimentari e Ambientali, Università della Basilicata, Viale dell'Ateneo Lucano 10, 85100 Potenza, Italy
[b] Instituto Pirenaico de Ecología (IPE-CSIC), Avda. Montañana 1005, E-50192 Zaragoza, Spain

ARTICLE INFO

Keywords:
EVI
Fraxinus ornus
Hydraulic diameter
NDVI
NDWI
Quercus pubescens

ABSTRACT

Drought reduces canopy cover, productivity and tree growth in forests. However, there is still little knowledge on how drought affects coupling between canopy greenness assessed by remote sensing and hydraulic conductivity detected by wood anatomy. This combination could improve the understanding of forest response to climate change. Thus, we investigated the impacts of a hot drought, which occurred in summer 2017, on radial growth, earlywood hydraulic diameter (Dh), a proxy of conductivity, and several remote-sensing indices in mixed Mediterranean hardwood forests (*Quercus pubescens* Willd. – *Fraxinus ornus L.*). In general, growth showed a higher coherence among trees and a higher responsiveness to climate. Growth decreased during the drought year, particularly for *Q. pubescens*, which showed high defoliation and dieback intensity. Both species showed a decline of Dh in 2018 after the drought and subsequent warm winter conditions. We found positive relationships between Dh and remote-sensing data for *Q. pubescens* in some of these vulnerable sites, where (i) growth was constrained by dry spring-summer conditions and (ii) Dh and growth covaried. These findings indicate a high variability among sites and tree species in their responses to drought considering earlywood anatomy, growth canopy cover and water content. However, some common patterns emerge such as links between potential hydraulic conductivity (Dh), tree cover and Dh-growth covariation in the most impacted sites. Further, *F. ornus* seem to perform better in terms of growth under drought conditions, showing less mortality and dieback than *Q. pubescens.* Future studies could explore how water transport and changes in canopy cover respond to dry and warm conditions and if that covariation indicates vulnerability to drought.

1. Introduction

Worldwide climate extremes such as droughts and heat waves are affecting forest ecosystems by reducing their productivity, cover and modifying their composition and structure, often triggering dieback episodes (Allen et al., 2015). Several tree-ring studies have evidenced a drought-related reduction of radial growth and resilience associated with a higher mortality risk (Gazol et al., 2018, DeSoto et al., 2020). Furthermore, droughts can cause changes in the wood anatomy by reducing the vessel lumen area and the hydraulic conductivity as has been observed in several ring-porous oak species (Corcuera et al., 2004, Colangelo et al., 2017). Thus, wood anatomical variables can record environmental signals including climate extremes (Fonti et al., 2010). Furthermore, wood anatomical variables such as the number and area (lumen) of vessels could be more meaningful and functional measures of post-drought resilience than tree-ring width (Schwarz et al., 2020). Using wood-anatomical variables such as lumen area or vessel density can allow overcoming some critical issues encountered when using tree-ring width to assess drought impacts such as different responses to spring or summer droughts between co-occurring species due to different xylem phenology or dynamics of use of stored carbon (Michelot et al., 2012).

However, several studies have noted that forests responses to climate events such as droughts depend on local factors such as site latitude, elevation, aspect, soil type and forest composition (Lloret et al., 2007, Rita et al., 2020). These studies have often assessed the impacts of droughts at continental to local scales using satellite-derived vegetation indices which are proxies of forest health, cover or greenness. Among

* Corresponding author.
E-mail addresses: santain.italiano@unibas.it (S.S.P. Italiano), jjcamarero@ipe.csic.es (J. Julio Camarero), borghetti@unibas.it (M. Borghetti), m.pizarro@csic.es (M. Pizarro), francesco.ripullone@unibas.es (F. Ripullone).

https://doi.org/10.1016/j.foreco.2023.121406
Received 21 June 2023; Received in revised form 30 August 2023; Accepted 3 September 2023
Available online 14 September 2023

these indices, one of the most widely used is the Normalized Different Vegetation Index (NDVI) (Rouse et al., 1973), which is very sensitive to photosynthetic activity and has been widely used to assess the health and productivity of drought-prone oak forests (e.g., Coluzzi et al., 2020, Khoury and Coomes, 2020; Vicente-Serrano et al., 2020). The NDVI was subsequently improved by developing the Enhanced Vegetation Index (EVI) (Huete et al., 1997), which reduces soil noise, atmospheric aerosols and the saturation of the reflectance signal at high levels of green biomass (Matsushita et al., 2007). The EVI has been widely used for investigating forest dieback allowing for an improved signal in thinned areas (Dionisio et al., 2012, Huang and Xia, 2019). It has been observed that forest growth and dieback are captured by the NDVI and EVI variability, at least in seasonally dry Mediterranean forests (Ogaya et al., 2015). To get information about water stress of vegetation the Normalized Difference Water Index (NDWI) was developed and used to estimate the water content of canopies and determining drought stress (Gao, 1996, Cheng et al., 2006, Sturm et al., 2022).

In addition to spatial variability, allocation shifts in stressed trees could lead to decoupled responses of canopy cover, growth and wood anatomy to climate (Mašek et al., 2023). Thus, the potential of remote sensing information to assess drought impacts on forests is evident, but it should be complemented by growth and wood anatomy data which may be more responsive proxies of drought stress (Gazol et al., 2018). Some studies have used tree ring and remote sensing series to better analyze the response of forests to extreme climate events such as droughts or frosts with variable results (Gazol et al., 2018, Moreno-Fernández et al., 2022, Tonelli et al., 2023, Vicente-Serrano et al., 2013, Wang et al., 2021); but few studies have yet compared remote sensing with wood anatomical variables such as earlywood vessel lumen area which provide sub-annual information (Fonti et al., 2010, Prendin et al., 2020).

This study aimed to analyze the responses of mixed hardwood forests to a severe drought by using radial growth, earlywood anatomy and remote-sensing indices (NDVI, EVI and NDWI). We assessed if these variables covary as a function of climatic variations in two coexisting porous-ring species (*Quercus pubescens*, *Fraxinus ornus*) vegetating in four sites characterized by different environmental conditions). By comparing the responses of these species, we sought to determine which of the proxies used (anatomical variables, vegetation indices) best highlight the impact of the drought event and thus which sites or species were most affected by the drought.

We expect that: (i) cover (e.g., NDVI, EVI) and growth (tree-ring width and area) variables would be positively related; and (ii) canopy water content (e.g., NDWI) and wood-anatomical variables related to hydraulic conductivity (e.g., earlywood hydraulic diameter) would be also positively related.

Given that *Q. pubescens* adopts a water-spending (anisohydric) strategy (Poyatos et al., 2008, Damesin and Rambal, 1995, Rosner, 2012), severe drought events could expose this species more to hydraulic collapse and dieback. *Fraxinus ornus*, on the other hand, seems to have a relatively isohydric strategy and shows a good control of reserves useful for rapid post-drought recovery (Tomasella et al., 2019). Indeed, *F. ornus* under conditions of reduced soil water availability, manages to allocate relatively more to leaf biomass and conductive phloem (Kiorapostolou and Petit, 2018) trying to counteract the impact of drought. Therefore, we expect the oak species (*Q. pubescens*) to be more sensitive and responsive to climatic stresses and changes in tree cover and greenery, in terms of growth and wood anatomy, than the ash species (*F. ornus*). Further, we expect to find the strongest associations between climate, cover-greenness variables (e.g., NDVI), growth (ring area) and wood anatomical variables in the most drought-stressed, least productive site. However, in colder sites we expect that the 2017 warm conditions would improve growth. Lastly, we also expect that comparing the response of *Q. pubescens* and *F. ornus* may provide useful insights into future trajectories of the Mediterranean forest community under climate change, with relevant management implications.

2. Material and methods

2.1. Study area

The study sites are mixed Mediterranean hardwood forests located in the Basilicata region, southern Italy (Fig. 1). Sites were selected because they showed damage after the 2017 extreme summer drought event (Fig. S1) with symptoms such as: leaf browning, premature leaf shedding, canopy dieback and elevated tree mortality (Coluzzi et al., 2020). Four sites with different productivity and environmental conditions where *Quercus pubescens* and *Fraxinus ornus* coexisted were selected. The sites presented different elevations, slopes and aspects (Table 1). They are located on sandstone substrates and clay soils.

Data from local meteorological stations close to the experimental sites were used to characterize the climatic conditions and variability (Table 1 and Table S1). The study area is subjected to Mediterranean climate conditions with warm and dry summers, cold winters and rainfall peaks in spring (March) and autumn (November). The Palazzo site (hereafter AP) located within the Accettura municipality territory is characterized by an average annual rainfall of 734 mm and an average annual temperature of 16 °C. The forest is a mixed oak-ash stand. The Ortosiderio site (hereafter OS), located within the Savoia di Lucania municipality territory, is also dominated by oak and ash with other minor hardwood species (*Crataegus orientalis* M. Bieb., *Quercus cerris* L. and *Ostrya carpinifolia* Scop). Here, the average annual rainfall is 889 mm and the average annual temperature is 13.0 °C. In this site, oak dieback was very evident with the highest mortality rate (61%) (Table 2). In the Pietrapertosa site (hereafter PI) *O. carpinifolia*, *C. orientalis* and *Pistacia terebinthus* L. are also found. The average annual rainfall is 671 mm and the average annual temperature is 12.7 °C. Lastly, in the Castelmezzano site (hereinafter CA), oak and ash co-occur with *Acer monspessulanum* L., *Cornus mas* L. and *P. terebinthus* and the climatic conditions are similar to those of the PI site. All experimental sites are generally even aged and high forests, with the exception of the AP site were high forest and coppice coexist, with this latter is being converted to high forest thanks to cessation of low coppice cuttings in the last decades. Indeed all these sites have been little or non exploited in the recent past because of difficulties to reach these locations.

2.2. Climate data and drought index

To calculate relationships between climate, growth, wood anatomy and remote sensing indices, as data from neighboring weather stations were too short and with heterogeneous time series (from 10 to 20 years), we used homogeneous, gap-filled climate series from the 0.1°-gridded EOBS climate dataset (v25.0e; Cornes et al., 2018). We obtained monthly data from April to September of mean, maximum and minimum temperatures and total precipitation for the 2001–2021 period. Although they have coarse spatial resolutions which do not allow for a detailed site-specific climate distinction, we selected this dataset because it provides long and homogeneous regional climate records. In addition, we also calculated the annual averages of temperature (MAT) and precipitation (MAP) for each site, using data records from local meteorological stations (Table 1 and Table S1).

Soil moisture was estimated for a 0–10 cm depth from the 0.1°-gridded NASA Land Data Assimilation Systems (LDAS, https://ldas.gsfc.nasa.gov/FLDAS/FLDASgoals.php). Lastly, we calculated the 0.1°-gridded Standardized Precipitation Evapotranspiration Index (SPEI), which is a multi-scalar drought index computed from monthly rainfall, temperature and potential evapotranspiration showing cumulative water surplus or deficit (Vicente-Serrano et al., 2010). We considered 12-month long SPEI values from April to September.

2.3. Field sampling

At each of the four study sites, a series of structural surveys were

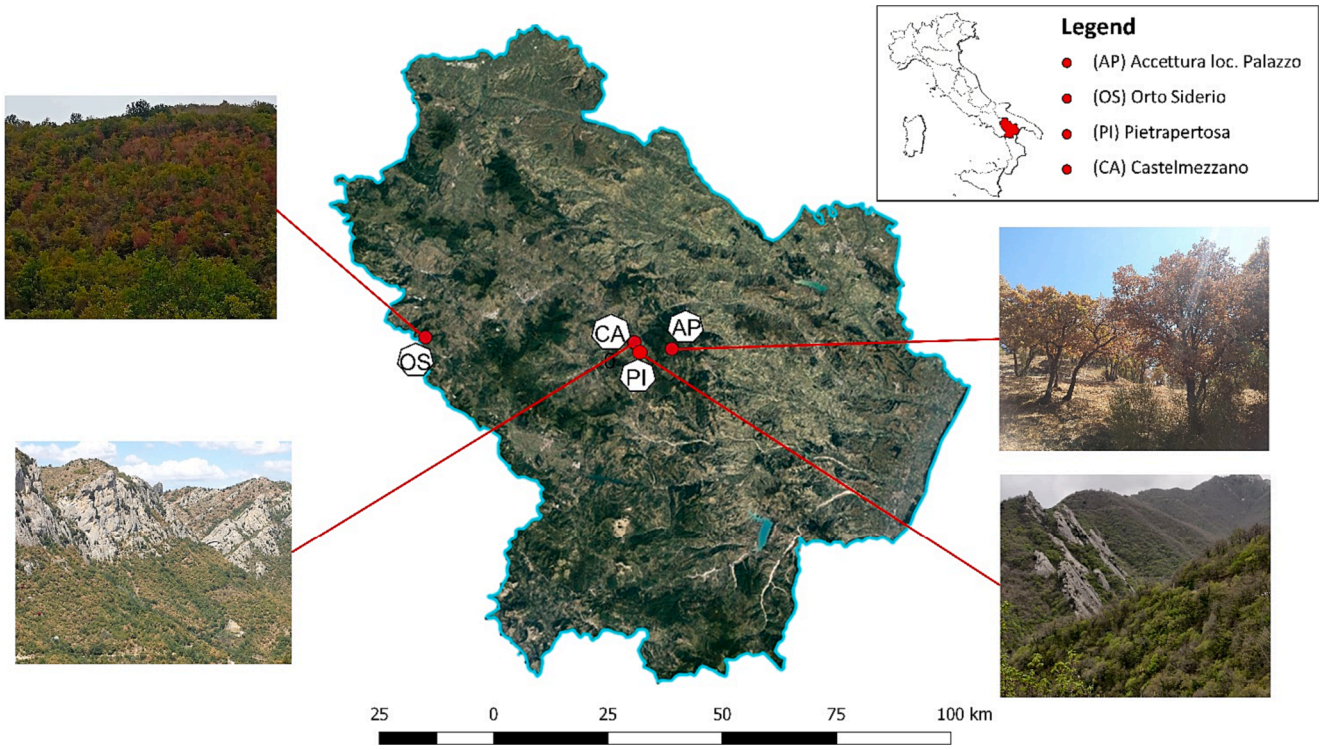

Fig. 1. Sites studied (OS, CA, PI and CA) located in the Basilicata region, southern Italy. The images show the impacts of the 2017 summer drought on the studied forests. See site codes in Table 1.

carried out in 2021. At each site, an area of 5000 m^2 (circular shape) was identified that was representative of the entire forest stand in terms of structure, composition and soil conditions. In each plot, all tree diameters at breast height (1.30 m), heights, plant status (living/dead) and the percentage of defoliation for each plant (crown transparency > 50% or < 50%) were measured (Dobbertin, 2005, Camarero et al., 2016). These measurements allowed to estimate for each stand tree density and basal area. Two transects of 50 m each were also carried out within each plot, along which it was possible to assess the projection of the crowns on the ground and thus the degree of canopy cover of each species. The assessment of the percentage cover was carried out not only to characterize each stand, but also to observe the canopy cover in the field and confirm the absence of clearings, rock formations or other types of cover other than tree crowns, which could have influenced or altered the remotely sensed vegetation indices.

2.4. Tree-ring width data

At each site, within each plot (5000 m^2), 15 dominant trees of each of the two representative species (oak, ash) were randomly sampled. Dominant trees have been selected as they form forest cover predominantly detected by satellite images and also because they are less affected on growth rings then submissive trees by competition for light, nutrients and water. Then 30 trees per site were sampled, for each of which two wood cores were taken at 1.3 m using a Pressler increment borer. Cores were air-dried, and their surfaces were cut using a sledge core microtome to clearly distinguish ring boundaries (Gärtner and Nievergelt, 2010). Tree rings were visually cross-dated under the binocular microscope by assigning characteristic rings (Fritts, 1976). Then, tree-ring widths were measured to the nearest 0.01 mm using the LINTAB package (Rinntech, Heidelberg, Germany). The COFECHA program (Holmes,1983) was used to evaluate the visual cross-dating of the tree-ring series by calculating moving correlations between individual series and the mean series of each species in each site.

2.5. Quantitative earlywood anatomy

We selected six trees per site and one radius per tree to perform anatomical analyses of ash and oak earlywood (hereafter EW). Selected trees were those showing the highest correlation between their indexed ring-width series and the mean site series. Wood anatomy was analyzed for the common 2001–2021 period.

Following Fonti et al. (2010) the surface of the cores was cleaned with high-pressure water blasting to remove both tyloses and wood dust from the vessel lumina. To improve the contrast, the vessel lumens were filled with white chalk powder. High resolution images of the rings (see Fig. S2) were captured at 20–40 magnification using a binocular and a camera (Zeiss Axiocam 208 color). The EW vessels were considered those with lumen diameters>50 μm and located in the first third section of the ring along the radial direction (Camarero et al., 2021). The EW lumen areas were measured in a tangential window of 2.5 mm using the ImageJ software (Schneider et al., 2012).

We quantified the following wood-anatomical traits following Scholz et al. (2013): ring area (mm^2), EW and latewood (LW) areas (mm^2), absolute and relative (%) areas occupied by vessels in the EW, EW vessel lumen area (μm^2) and vessel density. We also calculated two additional variables (*Dh* (μm), hydraulic diameter; *Kh* (kg m^{-1} s^{-1} MPa^{-1}), potential hydraulic conductivity) by considering the Hagen–Poiseuille lumen theoretical hydraulic conductivity for a vessel size (Tyree and Zimmermann, 2002).

The hydraulic diameter (*Dh*) for all EW vessels measured in each ring was the average of $\sum d^5/\sum d^4$, where *d* is the diameter of each EW vessel assuming a circular shape (Sperry et al., 1994). Lastly, the *Kh* of the EW was estimated as.

$$Kh = (\rho \times \pi \times \Sigma d^4) / (128 \times \mu \times Ar) \quad (1)$$

where ρ is the density of water at 20 °C (998.2 kg m^{-3} at 20 °C), d is the vessel lumen diameter, μ is the viscosity of water (1.002×10^{-9} MPa s at 20 °C) and *Ar* is the EW area imaged. We focused on EW vessels because they account for most of the ring hydraulic conductivity, particularly in

Table 1
Characteristics of the four study sites where Q. pubescens and F. ornus coexist and were sampled. MAT and MAP are the annual averages of temperature and precipitation for each site, obtained using data records from local meteorological stations (Table S1).

Site (code)	Longitude E	Latitude N	Elevation (m a.s.l.)	Slope (%)	Aspect	Substrate	MAT (°C)	MAP (mm)	Average temperature hottest month (July) (°C)	Average temperature coldest month (January) (°C)	Maximum temperaturehottest month (July2017) (°C)	Annual rainfall 2017 (mm)
Accettura Palazzo (AP)	16.148	40.516	790	15	W	Sandstone	16	734	26	7	39,6	548
Orto Siderio (OS)	15.546	40.573	600	35	N-NW	Clay	13	889	23	5	35,5	628
Pietrapertosa (PI)	16.058	40.533	625	35	N-NW	Sandstone	12,7	671	22	4	35	548
Castelmezzano (CA)	16.054	40.534	665	50	S-SE	Sandstone	12,7	671	22	4	35	548

the outermost ring in the case of ring-porous species (Ellmore and Ewers, 1985).

2.6. Remote sensing data

Analyses were performed using the Google Earth Engine platform (Gorelick et al., 2017) (https://earthengine.google.com, accessed 15 January 2023), for the 2001–2021 period, using Landsat scene collections for Top of the Atmosphere (TOA) reflectivity. A preliminary conversion from TOA scene reflectivity to surface reflectivity was performed, followed by atmospheric corrections and a cloudiness threshold of 40%. In addition, the data obtained from the different sensors (TM, ETM + and OLI) of the Landsat satellites (L5, L7, L8 and L9) were harmonised to obtain as much data as possible over the reference period (i.e. about 2880 spectral indexs values analyzed). The analysis for each study site was conducted on a representative forest stand area of 5000 m^2, i.e. the area involved in the field sampling. Using these data, three indices (NDVI, EVI, NDWI) were obtained (see the formulas in Table S2) with a spatial resolution of 30 m. The NDVI and EVI indices are used to characterize the canopy cover and photosynthetic activity, while the NDWI is used to examine the water content of the canopy. The indices were calculated at annual resolution or considering the seasons (prior winter, from December to February; spring, March to May; summer, June to August; autumn, September to November) or only the growing season (April to September).

Furthermore, using the Landsat image collections, we obtained the summer land surface temperature for each site (Ermida et al., 2020). To achieve this, we considered the wavelength of the thermal infrared bands (TIRS 1 and TIRS 2) with a spatial resolution of 100 m. In this way, we assessed the thermal emissivity of the soil to evaluate the impact of the 2017 drought on vegetation (Fig. S3).

2.7. Statistical analyses

Since the growth (ring area) and EW anatomy variables (Dh) used did not show any significant trend (Kendall τ tests, $p > 0.05$), we did not detrend their series which were averaged for each site and species. However, all annual or seasonal remote sensing indices showed significant positive trends ($p < 0.05$) due to the growth of tree cover and greenness over time. We removed these trends by fitting linear regression to the indices series and then subtracting observed minus fitted values so as to obtain residuals. To assess the changes in EW Dh between consecutive years we calculated ratios between the Dh of the current (year t) and previous (year/t) years in each site. Comparisons between sites or species were assessed using non-parametric Mann-Whitney tests.

Finally, to assess relationships between variables such climate, the SPEI drought index, Dh and remote-sensing indices we calculated Pearson correlations considering seasonal climatic values (mean temperatures and soil moisture; total precipitation) of the prior winter (December to February) and the growing season (April to September). Statistical analyses were done using the PAST software (Hammer et al., 2001).

3. Results

3.1. The 2017 drought and stand structure

Both the local climate data and the satellite-derived summer land surface temperature showed very dry and warm conditions in 2017, followed by warm conditions in 2018 (Figs. S1 and S3).

The lowest growing-season NDVI (0.67) and NDWI (0.20) values were found in site CA, whilst site AP showed the highest EVI (0.48) value (Table 2). Overall, the mortality rate was higher ($p = 0.03$) in oak (24%), particularly in site OS, than in ash (1%), but the basal area was also higher in the case of oak (19.2 vs 3.9 m^2/ha; $p = 0.03$).

Table 2
Structural and vegetation characteristics of the four stands analysed. Breast diameter values (dbh) are the mean ± SD of each species. Remote sensing indices are calculated for the growing season (April to September) and for the period 2001–2021.

Site	Sampled species	Stem density (Ind ha^{-1})	Dbh(cm)	Basal area (m^2 ha^{-1})	Dead trees in each species(%)	Crown defoliation 51–100% (%)	Canopy cover (%)	NDVI	EVI	NDWI
AP	*F. ornus*	220	16.0 ± 3.8	4.87	0	0	25	0.73	0.48	0.25
	Q. pubescens	580	19.0 ± 6.6	18.06	0	45	72			
OS	*F. ornus*	560	9.0 ± 3.2	3.96	0	7	60	0.74	0.45	0.29
	Q. pubescens	720	18.0 ± 6.8	20.88	61	89	35			
PI	*F. ornus*	300	7.0 ± 0.7	0.82	0	0	40	0.74	0.45	0.26
	Q. pubescens	1300	14.0 ± 5.1	23.39	11	45	62			
CA	*F. ornus*	1260	8.0 ± 2.4	5.97	3	10	66	0.67	0.45	0.20
	Q. pubescens	640	16.0 ± 6.5	14.56	19	84	45			

3.2. Growth and EW anatomy responses to the 2017 drought

The annual ring area was similar between *Q. pubescens* (2.4 mm^2) and *F. ornus* (2.2 mm^2) (Table 3). A similar result was found for the EW (1.1 vs. 0.8 mm^2) and LW areas (1.3 vs. 1.4 mm^2). Both the EW Dh and Kh were higher ($p = 0.02$) in *Q. pubescens* (286 μm, 12.2 10^{-10} Kg m^{-1} s^{-1} MPa^{-1}) than in *F. ornus* (146 μm, 1.9 10^{-10} Kg m^{-1} s^{-1} MPa^{-1}). The highest Dh and Kh values were found for *Q. pubescens* in sites AP and OS, and the lowest Dh and Kh values for *F. ornus* from OS site (Table 3).

The mean Dh series of *Q. pubescens* and *F. ornus* were positively correlated in three out of the four study sites (AP, $r = 0.60$, $p = 0.004$; PI, $r = 0.65$, $p = 0.001$; CA, $r = 0.56$, $p = 0.008$), whereas the ring-area series were not significantly correlated in any study site.

In 2017, the ring area of both tree species dropped in OS and PI sites (Fig. 2). In OS, both species recovered ring area values in 2018. Regarding the EW Dh, it decreases in 2018 in all sites, particularly in the case of *Q. pubescens* (Fig. 3). The Dh reduction in 2018 was the strongest in site PI and the weakest in site CA (Fig. S4). There were positive and significant relations between ring area and EW Dh in the case of *Q. pubescens* in sites AP, OS and CA and in the case of *F. ornus* in site OS (Fig. 4).

Lastly, the within-site coherence (Pearson correlations) among individual series of ring-area was higher than that among individual series of EW Dh in the case of *Q. pubescens* (0.61 mm^2 vs. 0.27 μm, $p = 0.02$) and also in the case of *F. ornus* (0.45 mm^2 vs. 0.15 μm, $p = 0.03$) (Table S3). The mean coherence of Dh series was high (0.41) only in site PI and in the case of *Q. pubescens*, whereas in the case of ring area it peaked in site AP and also for *Q. pubescens* (0.74).

3.3. Relationships between growth, wood anatomy and remote-sensing indices

We detected drops of the prior-winter and the growing-season NDVI in 2017–2018 in site OS, but the growing-season NDWI increased in site AP (Fig. 5). In site AP, the growing-season NDWI and the *Q. pubescens* ring area were positively related (Fig. 5a). In site OS, the *Q. pubescens* EW Dh was positively correlated with the prior-winter NDVI (Fig. 5b) and the growing-season EVI (Fig. 5c).

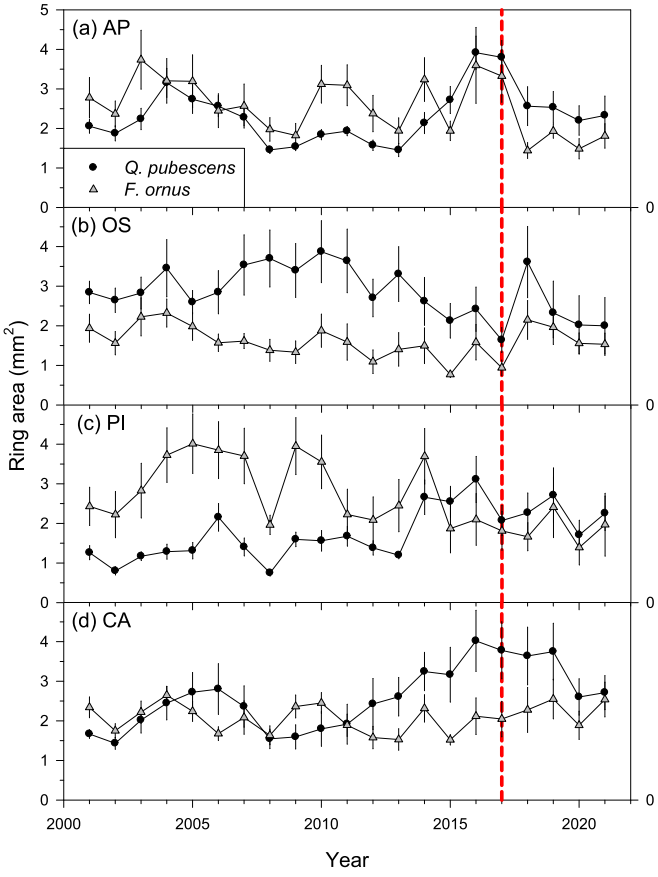

Fig. 2. Ring area values measured for *Q. pubescens* and *F. ornus* in the four study sites (AP, OS, PI and CA). The dashed vertical line shows the 2017 drought. Values are means ± SE.

Table 3
Mean growth and anatomical variables calculated for each species and study site. The dbh values are means ± SD of the six trees sampled per site of each species. Values of ring area, earlywood (EW) and latewood (LW) area, hydraulic diameter (Dh) and hydraulic conductivity (Ks) are also means ± SD calculated for the common period 2001–2021.

Site	Species	Dbh (cm)	Ring area (mm^2)	EW area (mm^2)	LW area (mm^2)	Dh (μm)	Kh * 10^{-10} (Kg m^{-1} s^{-1} MPa^{-1})
AP	*F. ornus*	17.0 ± 3.3	2.54 ± 0.71	0.96 ± 0.14	1.58 ± 0.59	167.0 ± 8.8	2.81 ± 0.41
	Q. pubescens	19.0 ± 4.2	2.30 ± 0.70	1.30 ± 0.25	1.01 ± 0.52	307.5 ± 16.2	16.74 ± 4.97
OS	*F. ornus*	8.0 ± 2.3	1.61 ± 0.40	0.63 ± 0.10	0.98 ± 0.32	128.9 ± 5.9	1.15 ± 0.31
	Q. pubescens	26.0 ± 8.2	2.88 ± 0.67	1.22 ± 0.16	1.46 ± 0.50	306.4 ± 20.0	16.28 ± 3.90
PI	*F. ornus*	10.0 ± 1.6	2.72 ± 1.00	0.91 ± 0.19	1.80 ± 0.83	138.7 ± 7.3	1.76 ± 0.34
	Q. pubescens	17.0 ± 4.4	1.76 ± 0.65	0.80 ± 0.15	0.96 ± 0.53	249.1 ± 17.0	5.92 ± 1.88
CA	*F. ornus*	11.0 ± 2.5	2.06 ± 0.39	0.85 ± 0.07	1.21 ± 0.34	149.4 ± 7.3	1.75 ± 0.33
	Q. pubescens	21.0 ± 4.9	2.66 ± 0.93	1.01 ± 0.17	1.65 ± 0.77	281.1 ± 14.0	9.78 ± 2.68

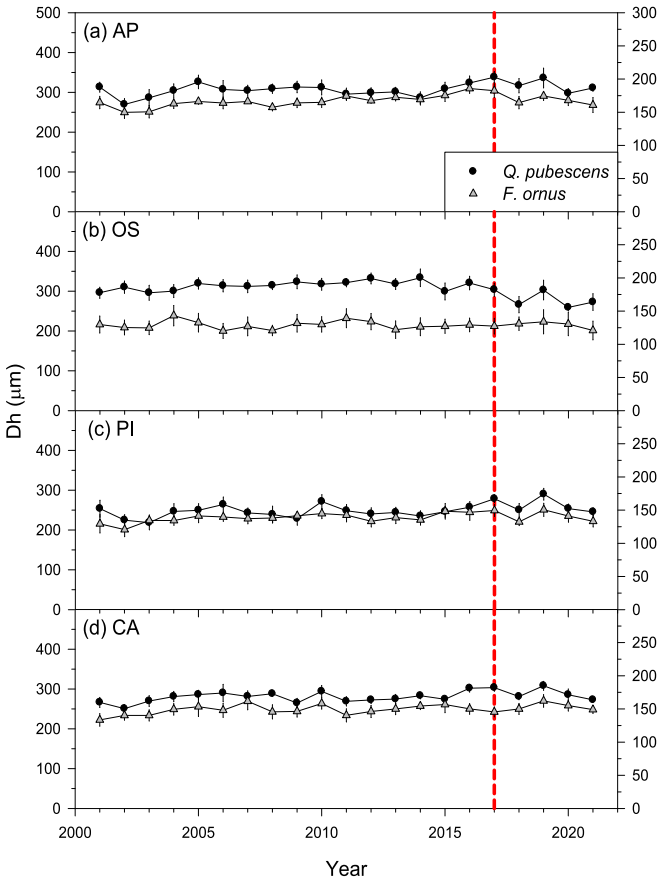

Fig. 3. Earlywood hydraulic diameters (*Dh*) for *Q. pubescens* and *F. ornus* in the four study sites. The dashed vertical line shows the 2017 drought. Values are means ± SE.

3.4. Relationships between climate, growth, earlywood anatomy and remote-sensing indices

Radial growth was enhanced by wet-cool conditions in spring and summer in *Q. pubescens* from sites OS and CA and *F. ornus* from site PI (Table 4). Warm prior autumn to winter conditions also improved *Q. pubescens* growth. In sites OS and PI, a high spring-summer SPEI was positively related to *F. ornus* growth. The EW Dh of both species was enhanced by cool prior December conditions (Table 4). In sites CA, PI and OS, the EW Dh of *F. ornus* increased in response to wet conditions from February to May.

Few significant correlations, and only in some sites, were found when relating climate variables, including the SPEI, and the remote-sensing indices. In site OS, the NDVI and the EVI showed positive relationship with the April-September precipitation ($r = 0.52$, $p = 0.02$ and $r = 0.55$, $p = 0.009$, respectively). Only in this site we found a positive association between prior-winter precipitation and the NDVI ($r = 0.42$, $p = 0.04$). In the same site, the May and June soil moisture were positively related to the NDWI ($r = 0.46$, $p = 0.05$) and NDVI ($r = 0.52$, $p = 0.02$) series, respectively. Again in site OS, the June maximum temperature negatively correlated with the NDVI ($r = -0.54$, $p = 0.01$) and the NDWI ($r = -0.66$, $p = 0.002$). In site AP, the growing season NDVI ($r = -0.46$, $p = 0.05$) and the EVI ($r = -0.69$, $p = 0.001$) were negatively related to the 12-month SPEI, whereas in site PI the April NVWI was negatively correlated with the SPEI ($r = -0.50$, $p = 0.04$).

4. Discussion

Overall, the associations observed between climate, growth, earlywood anatomy and remote-sensing indices were contingent on site conditions and species' characteristics. Similar results have been found in a previous paper at larger scale in Mediterranean environment (Rita et al., 2020). Indeed, the impact of summer drought greatly depended on site conditions since elevation, exposure and vegetation type influence this response. These diverse relationships indicate that the impact of the 2017 drought on forest growth and productivity was heterogeneous. For instance, the growth drop due to the 2017 drought was evident in some sites (e.g., site OS) but not in others (e.g., site AP). The fact that in AP growth declined in 2018 could be likely related to a delated response to the summer 2017 drought. Furthermore, in this site, wet winter-spring conditions improved *Q. pubescens* growth, allowing trees to grow abundantly before the summer drought arrives. This was also shown by the positive relationship to the growing-season NDWI, that can be explained by the high oak cover of this site, which was dominated by *Q. pubescens*. This finding emphasizes the need of a reliable description of stand structure and composition when analyzing mixed forests using remote-sensing information.

Interestingly, the most impacted site OS also presented: (i) the highest percentage of dead *Q. pubescens* trees, (ii) a strong covariation between growth and earlywood hydraulic diameter (EW Dh) of both species, and (iii) positive associations between the EW Dh of *Q. pubescens* and remote-sensing indices (EVI, NDVI). Indeed, this site with relatively high slope and clay soils was probably the most vulnerable to the negative impacts of the 2017 summer hot drought. Nevertheless, although more sensitive, site OS was not the least productive site, as expected, according to remote-sensing data. This is most likely due to the fact that the remotely sensed data returns an average value of the entire mixed stand. Thus, the ash tree, which was already present with a developed canopy in the dominated strip of the forest, as a result of the death or desiccation of the oak tree canopies, still maintained the green cover (as an underlying green layer) by exploiting the available light gaps. This could be the reason why the remote sensing indices did not perceive significant reductions in greenness compared to the other sites.

We found a reduction of the 2018 EW Dh in three out of the four study sites (AP, OS and PI). In the most vulnerable site OS, this post-drought reduction was also observed in the NDVI and EVI. Such carry-over could have been caused by the warm conditions during the 2017–2018 winter leading to smaller earlywood vessels in 2018. In previous studies on Mediterranean oaks, both a low coherence among trees and a negative association between winter temperatures and EW Dh were also found (Alla and Camarero, 2012). Such decrease in Dh led to a reduced potential hydraulic conductivity in 2018 which was not translated into reduced radial growth, therefore confirming a high recovery capacity of the study stands.

This recovery capacity has been observed in other drought-prone Mediterranean stands (Gazol et al., 2018) and could be due to post-drought thinning to alterations in stand structure and composition due to the death or defoliation of the canopy of the most affected sites (e.g. the OS site) (Coluzzi et al., 2020).

The results presented suggest a probable reorganisation and improved response of *F. ornus* at sites such as OS and CA, where *Q. pubescens* showed greater defoliation, but surviving oak trees also showed a high resumption of growth after drought. At these more affected sites, the increased dieback and death of *Q. pubescens* may have reduced competition for water and soil nutrients in favour of surviving conspecifics and *F. ornus*. Furthermore, the reduction in competitors may not only favour the availability of resources for the individuals that have tolerated the disturbance, but also allow for an increase in the drought resistance of forest stands.

These responses depend not only on site characteristics (Rita et al., 2020), but also on forest structure and stand composition (Lloret et al., 2007). As expected, *Q. pubescens* was more responsive to climate and changes in tree cover and greenness (higher growth-Dh covariation, higher correlations with NDVI, EVI and NDWI than *F. ornus*, excepting the high growth-SPEI correlations found in site PI). A similar growth-Dh

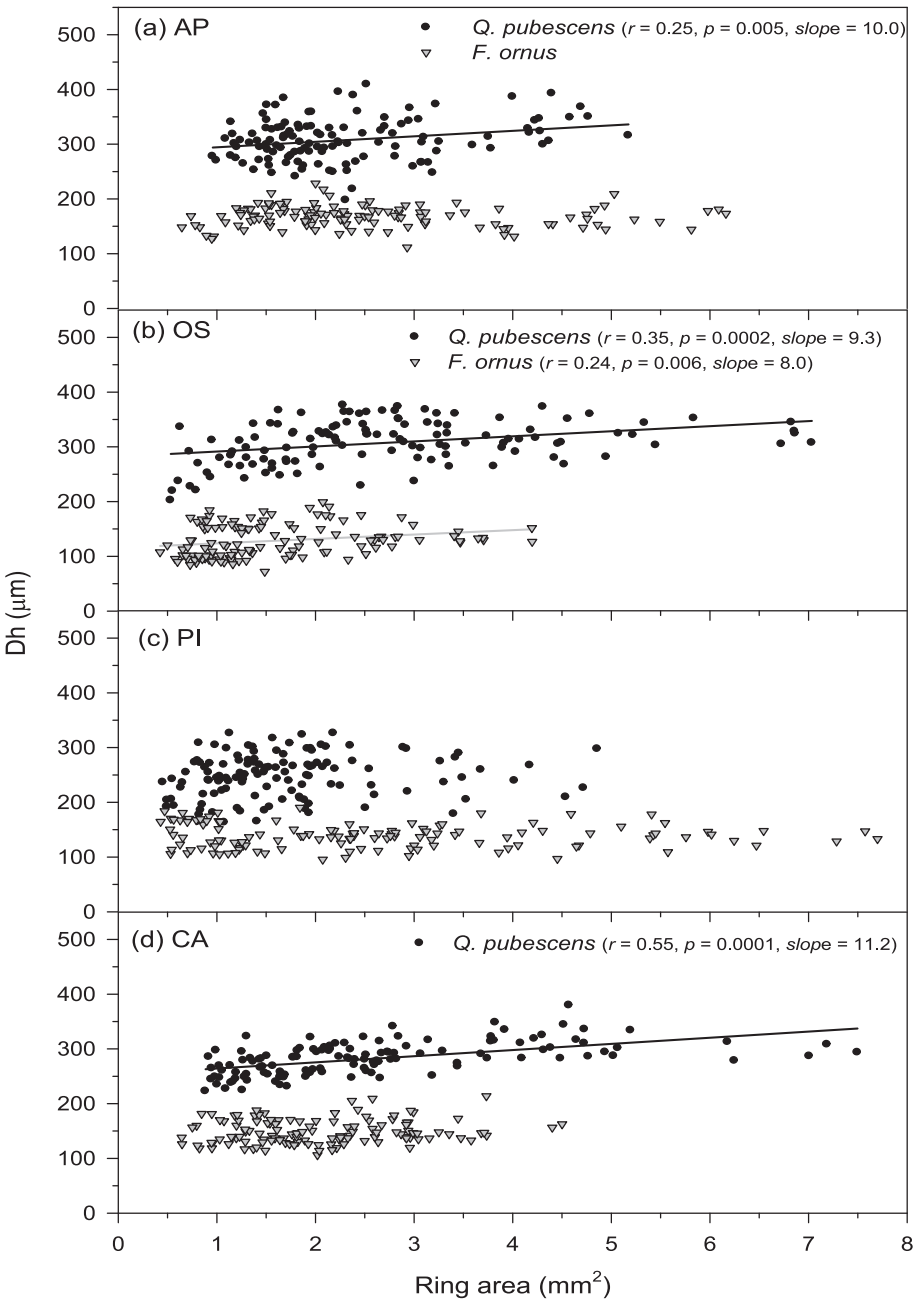

Fig. 4. Relationships between ring area and the earlywood hydraulic diameter (*Dh*) in the four study sites. Lines show significant ($p < 0.05$) linear regressions between both variables. Statistics show the correlation coefficients (*r*), its significance level (*p*) and the slopes of regressions.

covariation has also been observed in other ring-porous tree species (Camarero et al., 2021), and it has been hypothesised that significant deviations of the growth-anatomy covariation could indicate stress conditions.

In less impacted sites such as AP, *Q. pubescens* could have formed most of their ring before the 2017 drought onset or it may have relied more on stored non-structural carbohydrates than *F. ornus* to grow (Colangelo et al., 2017). The temporal mismatch between growth phenology (xylogenesis) and drought timing influences growth legacies and could explain these different responses (Camarero et al., 2015, Camarero et al., 2018, Huang et al., 2018). Such carry-over effects and/or the occurrence of compound climate events (in our case, drought followed by a warm winter) would also explain the reduction in the 2018 vessel lumen area. In addition, different carbon allocation patterns could explain differences between coexisting species. For example, *F. ornus* allocates more carbon to leaf biomass and phloem to compensate for the negative impacts of reduced soil water availability on stomatal conductance (Kiorapostolou and Petit, 2018). In addition, embolism phenomena leading to tree desiccation and dieback should also be investigated. Not only drought but also the increase in CO_2 would seem to influence xylem embolism phenomena in different forest species (Tognetti et al. 1999), e.g. significant effects of high CO_2 concentrations on the loss of hydraulic conductivity were observed in *Q. pubescens*, while the response was less pronounced in *F. ornus*.

4.1. Management implications

Adaptive forest management could be used for managing dieback stands through targeted and flexible interventions on the stand structure, composition and regeneration (Gentilesca et al., 2017). By

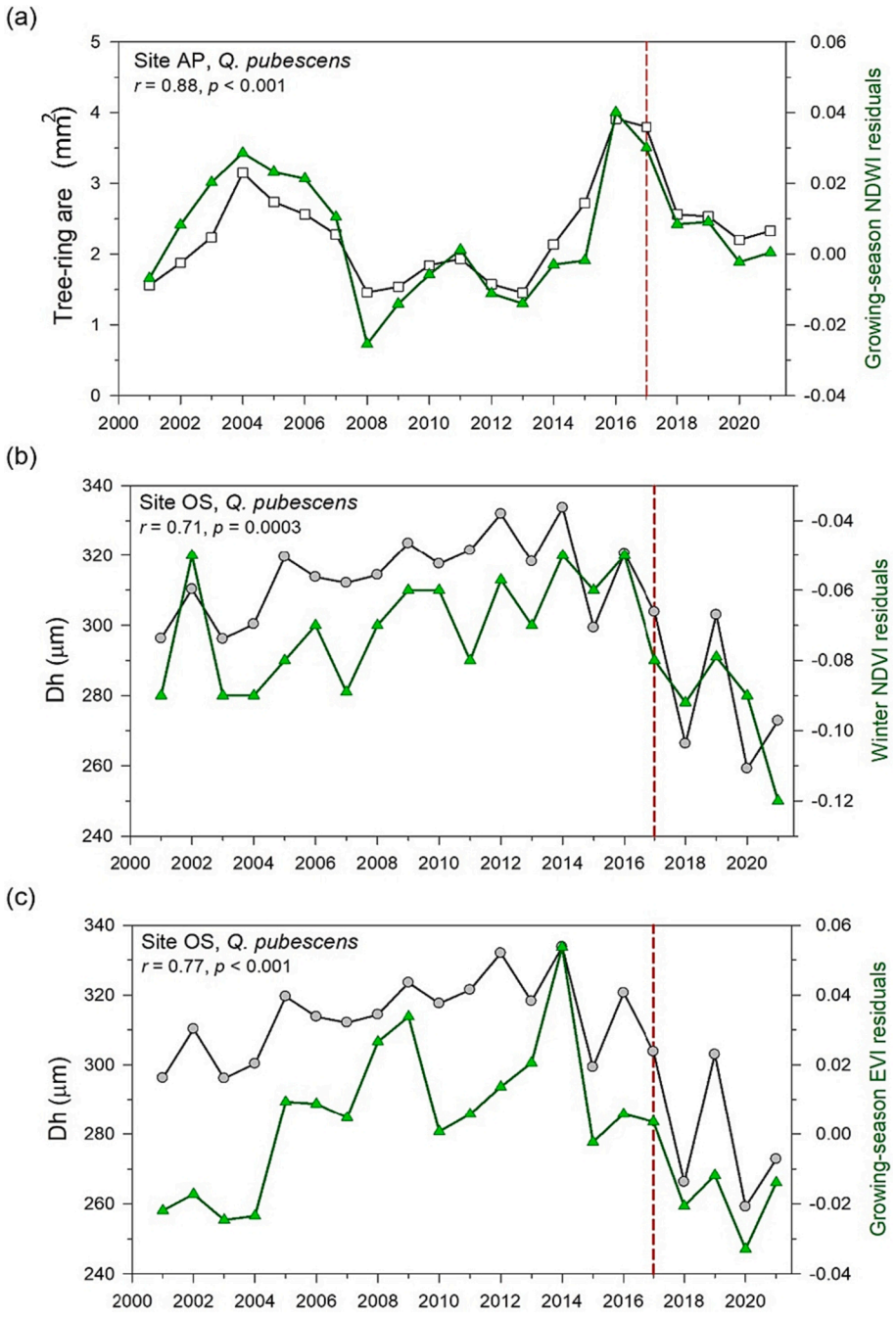

Fig. 5. Main relationships found between remote-sensing variables and ring area (a) or hydraulic diameter (*Dh*) (b and c). The dashed vertical line indicates the 2017 drought.

reducing competition and structural homogeneity and by promoting biodiversity, forests could be less vulnerable to drought (Borghetti, 2012). Useful actions, at the early stages of dieback with widespread defoliation, would be interventions on understory vegetation to increase the available soil moisture. This attempts to retain water in the soil and promote the degradation of organic matter and nutrient availability. Selective thinning could be performed to increase resilience by reducing intra- and inter-specific competition (Gentilesca et al., 2017), favouring selected trees which better recover after drought. Thus, in our case, action should be taken to reduce stand density but also to favour *Q. pubescens* (with greater defoliation and mortality rates than *F. ornus*) in order to maintain the composition of the mixed forest and to improve forest resilience. Furthermore, for highly degraded sites, regeneration should be encouraged, and the production of viable seed should be enhanced. Therefore, regeneration cuts should be anticipated in order to replace declining trees with young trees that are more resistant to stress events and with higher viable seed production.

5. Conclusions

We analyzed the impacts of a hot summer drought on growth, earlywood anatomy (hydraulic diameter) and remote-sensing indices (NDVI, EVI and NDWI) in mixed hardwood forests. We found disparate responses depending on site conditions and the considered species. At all sites, the species analysed showed a reduction in ring area as a consequence of the 2017 drought extreme event. This reduction in growth was less evident at the AP site, which is located at a higher altitude and therefore probably experienced the heat wave later than the other

Table 4
Pearson correlations between ring area or hydraulic diameter (Dh) and climate variables (period 2001–2021). Months abbreviated by lower- and upper-case letters correspond to the prior and current years, respectively. Only significant ($p < 0.05$) coefficients are presented.

Site AP, Ring area													Site OS, Ring area											
Maximum temperature	o	n	d	J	F	M	A	M	J	J	A	S	Maximum temperature	o	n	d	J	F	M	A	M	J	J	A	S
Q. pubescens		0.50											*Q. pubescens*	0.46											
F. ornus													*F. ornus*												
Minimum temperature													Minimum temperature												
Q. pubescens	0.46												*Q. pubescens*	0.66	0.62										
F. ornus													*F. ornus*												
Precipitation													Precipitation												
Q. pubescens			0.49				0.47						*Q. pubescens*								0.55	0.46			
F. ornus			0.58										*F. ornus*												
Soil moisture													Soil moisture												
Q. pubescens													*Q. pubescens*							0.50	0.49	0.55			
F. ornus													*F. ornus*												
SPEI6													SPEI6												
Q. pubescens													*Q. pubescens*									0.47	0.57		
F. ornus	0.57												*F. ornus*											0.52	0.51
Site AP, Dh													Site OS, Dh											
Maximum temperature	o	n	d	J	F	M	A	M	J	J	A	S	Maximum temperature	o	n	d	J	F	M	A	M	J	J	A	S
Q. pubescens			−0.58										*Q. pubescens*			−0.48									
F. ornus			0.68										*F. ornus*			−0.46									
Minimum temperature													Minimum temperature												
Q. pubescens			−0.51										*Q. pubescens*												
F. ornus			−0.56										*F. ornus*												
Precipitation													Precipitation												
Q. pubescens													*Q. pubescens*												
F. ornus													*F. ornus*							0.47					
Soil moisture													Soil moisture												
Q. pubescens													*Q. pubescens*												
F. ornus		0.52											*F. ornus*								0.48				
SPEI6													SPEI6												
Q. pubescens													*Q. pubescens*												
F. ornus													*F. ornus*												
Site CA, Ring area													Site PI, Ring area											
Maximum temperature	o	n	d	J	F	M	A	M	J	J	A	S	Maximum temperature	o	n	d	J	F	M	A	M	J	J	A	S
Q. pubescens			0.60										*Q. pubescens*		0.46	0.62									
F. ornus													*F. ornus*												
Minimum temperature													Minimum temperature												
Q. pubescens							0.50						*Q. pubescens*					0.49							
F. ornus													*F. ornus*						0.51					−0.55	
Precipitation													Precipitation												
Q. pubescens													*Q. pubescens*												
F. ornus													*F. ornus*												
Soil moisture													Soil moisture												
Q. pubescens													*Q. pubescens*												

(*continued on next page*)

Table 4 (*continued*)

F. ornus													*F. ornus*						0.64				0.48			
SPEI6													SPEI6													
Q. pubescens													*Q. pubescens*													
F. ornus													*F. ornus*						0.73	0.80	0.72	0.67	0.56			
Site CA, Dh													Site PI, Dh													
Maximum temperature	o	n	d	J	F	M	A	M	J	J	A	S	Maximum temperature	o	n	d	J	F	M	A	M	J	J	A	S	
Q. pubescens			−0.58										*Q. pubescens*			−0.58										
F. ornus			−0.47										*F. ornus*			−0.62										
Minimum temperature													Minimum temperature													
Q. pubescens			−0.46										*Q. pubescens*			−0.46										
F. ornus													*F. ornus*			−0.49										
Precipitation													Precipitation													
Q. pubescens													*Q. pubescens*													
F. ornus					0.47								*F. ornus*													
Soil moisture													Soil moisture													
Q. pubescens													*Q. pubescens*													
F. ornus						0.48							*F. ornus*						0.55							
SPEI6													SPEI6													
Q. pubescens													*Q. pubescens*													
F. ornus													*F. ornus*													

stands. At this site, the trees probably took advantage of the non-structural carbohydrates for radial growth during the drought and then suffered the disturbance in the following year, unlike all the other sites.

Furthermore, looking at the local climatic data (Table 1), we see that the AP site, despite being located at a higher altitude, is the warmest site, with higher average temperatures than the other sites and higher maximum temperatures reached in 2017. It is probably also for this reason that in 2017 the plants at the AP site did not show sharp drops in performance (reduction in ring area) as at other sites, because the stand may have already adapted over time to warmer thermal conditions.

While a year after the drought a general decline in Dh was observed, probably as a consequence of dry summer conditions followed by a warm winter more evident for *Q. pubescens*. Overall, the data obtained seem to indicate a better condition of *F. ornus* than *Q. pubescens* even in the most impacted sites. Indeed drought resistant ash species may progressively outcompete more mesic oak species in the mixed Mediterranean forest under a drought-prone climate, with relevant effects for forest management and ecosystem services at the landscape scale. The information obtained from our study will be useful in improving our understanding of the relationships between growth, wood anatomy and remote sensing and will allow us to supplement our knowledge of the understudied *F. ornus*. Further research could consider investigating how changes in stand composition or structural diversity influence tree growth, wood anatomy and forest productivity and how these changes determine forest vulnerability to drought.

CRediT authorship contribution statement

Santain S.P. Italiano: Conceptualization, Data curation, Formal analysis, Investigation, Methodology, Writing – original draft, Writing – review & editing. **J. Julio Camarero:** Data curation, Formal analysis, Funding acquisition, Supervision, Validation, Writing – original draft, Writing – review & editing. **Marco Borghetti:** Funding acquisition, Supervision, Visualization, Writing – review & editing. **Michele Colangelo:** Methodology, Writing – review & editing. **Manuel Pizarro:** Formal analysis, Validation, Writing – review & editing. **Francesco Ripullone:** Conceptualization, Funding acquisition, Investigation, Methodology, Supervision, Visualization, Writing – review & editing.

Declaration of Competing Interest

The authors declare that they have no known competing financial interests or personal relationships that could have appeared to influence the work reported in this paper.

Data availability

Data will be made available on request.

Acknowledgments

The Italian Ministry of University has supported this research in the framework of the project ARS01_00405, “OT4CLIMA, Advanced EO technologies for studying Climate Change impacts on the environment” (D.D. 2261 del 6.9.2018, PON R & I 2014-2020 and FSC). This study was also supported within the Agritech National Research Center and partially financed by the European Union Next-GenerationEU (Piano Nazionale di Ripresa e Resilienza (PNRR) – Missione 4 Componente 2, Investimento 1. 4 – D.D. 1032 17 /06 /2022CN00000022). JJC acknowledges support of the project CGL2015-69186-C2-1-R (Spanish Ministry of Science. We acknowledge the E-OBS dataset from the EU-FP6 project UERRA (http://www.uerra.eu) and the Copernicus Climate Change Service, and the data providers in the ECA&D project (https://www.ecad.eu).

Appendix A. Supplementary data

Supplementary data to this article can be found online at https://doi.org/10.1016/j.foreco.2023.121406.

References

Alla, A.Q., Camarero, J.J., 2012. Contrasting responses of radial growth and wood anatomy to climate in a Mediterranean ring-porous oak: implications for its future persistence or why the variance matters more than the mean. Eur. J. For. Res. 131, 1537–1550. https://doi.org/10.1007/s10342-012-0621-x.

Allen, C.D., Breshears, D.D., McDowell, N.G., 2015. On underestimation of global vulnerability to tree mortality and forest die-off from hotter drought in the Anthropocene. Ecosphere 6, 129. https://doi.org/10.1890/ES15-00203.1.

Borghetti, M., 2012. Principi fondanti, mosaico delle conoscenze e selvicoltura adattativa. Forest@-Journal of Silviculture and Forest. Ecology 9 (4), 166. https://doi.org/10.3832/efor0699-009.

Camarero, J.J., Franquesa, M., Sangüesa-Barreda, G., 2015. Timing of drought triggers distinct growth responses in holm oak: implications to predict warming-induced forest defoliation and growth decline. Forests 6, 1576–1597. https://doi.org/10.3390/f6051576.

Camarero, J.J., Sangüesa-Barreda, G., Vergarechea, M., 2016. Prior height, growth, and wood anatomy differently predispose to drought-induced dieback in two Mediterranean oak species. Ann. For. Sci. 73, 341–351. https://doi.org/10.1007/s13595-015-0523-4.

Camarero, J.J., Gazol, A., Sangüesa-Barreda, G., Cantero, A., Sánchez-Salguero, R., Sánchez-Miranda, A., Granda, E., Serra-Maluquer, X., Ibáñez, R., 2018. Forest growth responses to drought at short- and long-term scales in Spain: squeezing the stress memory from tree rings. Front. Ecol. Evol. 6 https://doi.org/10.3389/fevo.2018.00009.

Camarero, J.J., Colangelo, M., Rodríguez-González, P.M., Sánchez-Miranda, A., Sánchez-Salguero, R., Campelo, F., Rita, A., Ripullone, F., 2021. Wood anatomy and tree growth covary in riparian ash forests along climatic and ecological gradients. Dendrochronologia 70. https://doi.org/10.1016/j.dendro.2021.125891, 125891.

Cheng, Y.B., Zarco-Tejada, P.J., Riaño, D., Rueda, C.A., Ustin, S.L., 2006. Estimating vegetation water content with hyperspectral data for different canopy scenarios: Relationships between AVIRIS and MODIS indexes. Remote Sens. Environ. 105, 354–366. https://doi.org/10.1016/j.rse.2006.07.005.

Colangelo, M., Camarero, J.J., Battipaglia, G., Borghetti, M., De Micco, V., Gentilesca, T., Ripullone, F., 2017. A multi-proxy assessment of dieback causes in a Mediterranean oak species. Tree Physiol. 37, 617–631. https://doi.org/10.1093/treephys/tpx002.

Coluzzi, R., Fascetti, S., Imbrenda, V., Italiano, S.S.P., Ripullone, F., Lanfredi, M., 2020. Exploring the Use of Sentinel-2 Data to Monitor Heterogeneous Effects of Contextual Drought and Heatwaves on Mediterranean Forests. Land 9, 325. https://doi.org/10.3390/land9090325.

Corcuera, L., Camarero, J.J., Gil-Pelegrín, E., 2004. Effects of a severe drought on growth and wood-anatomical properties of *Quercus faginea*. IAWA J. 25 (2), 185–204.

Cornes, R.C., van der Schrier, G., van den Besselaar, E.J.M., Jones, P.D., 2018. An ensemble version of the E-OBS temperature and precipitation data sets. J. Geophys. Res. Atm. 123, 9391–9409. https://doi.org/10.1029/2017JD028200.

Damesin, C., Rambal, S., 1995. Field study of leaf photosynthetic performance by a Mediterranean deciduous oak tree (*Quercus pubescens*) during a severe summer drought. New Phytol. 131 (2), 159–167. https://doi.org/10.1111/j.1469-8137.1995.tb05717.x.

DeSoto, L., Cailleret, M., Sterck, F., Jansen, S., Kramer, K., Robert, E.M.R., Martínez-Vilalta, J., 2020. Low growth resilience to drought is related to future mortality risk in trees. Nat. Commun. 11, 545. https://doi.org/10.1038/s41467-020-14300-5.

Dionisio, M.A., Alcaraz-Segura, D., Cabello, J., 2012. Satellite-based monitoring of ecosystem functioning in protected areas: recent trends in the oak forests (*Quercus pyrenaica* Willd.) of Sierra Nevada (Spain). International Perspectives on. Glob. Environ. Chang. 355, 37.

Dobbertin, M., 2005. Tree growth as indicator of tree vitality and of tree reaction to environmental stress: a review. Eur. J. For. Res. 124, 319–333. https://doi.org/10.1007/s10342-005-0085-3.

Ellmore, G.S., Ewers, F.W., 1985. Hydraulic conductivity in trunk xylem of elm. *Ulmus americana*. IAWA journal Bull. 6 (4), 303–307.

Ermida, S.L., Soares, P., Mantas, V., Göttsche, F.M., Trigo, I.F., 2020. Google Earth Engine open-source code for land surface temperature estimation from the Landsat series. Remote Sens. 12, 1471. https://doi.org/10.3390/rs12091471.

Fonti, P., von Arx, G., García-González, I., Eilmann, B., Sass-Klaassen, U., Gärtner, H., Eckstein, D., 2010. Studying global change through investigation of the plastic responses of xylem anatomy in tree rings. New Phytol. 185, 42–53. https://doi.org/10.1111/j.1469-8137.2009.03030.x.

Fritts, H.C., 1976. Tree Rings and Climate. Academic Press, London.

Gao, B.C., 1996. NDWI–A normalized difference water index for remote sensing of vegetation liquid water from space. Remote Sens. Environ. 58, 257–266. https://doi.org/10.1016/S0034-4257(96)00067-3.

Gärtner, H., Nievergelt, D., 2010. The core-microtome: a new tool for surface preparation on cores and time series analysis of varying cell parameters. Dendrochronologia 28, 85–92. https://doi.org/10.1016/j.dendro.2009.09.002.

Gazol, A., Camarero, J.J., Vicente-Serrano, S.M., Sánchez-Salguero, R., Gutiérrez, E., de Luis, M., Sangüesa-Barreda, G., Novak, K., Rozas, V., Tíscar, P.A., Linares, J.C., Martín-Hernández, N., Martínez del Castillo, E., Ribas, M., García-González, I., Silla, F., Camisón, A., Génova, M., Olano, J.M., Longares, L.A., Hevia, A., Tomás-Burguera, M., Galván, J.D., 2018. Forest resilience to drought varies across biomes. Glob. Chang. Biol. 24 (5), 2143–2158.

Gentilesca, T., Camarero, J.J., Colangelo, M., Nolè, A., Ripullone, F., 2017. Drought induced oak decline in the western Mediterranean region: an overview on current evidences, mechanisms and management options to improve forest resilience. IForest 10 (5), 796–806. https://doi.org/10.3832/ifor2317-010.

Gorelick, N., Hancher, M., Dixon, M., Ilyushchenko, S., Thau, D., Moore, R., 2017. Google Earth Engine: Planetary-scale geospatial analysis for everyone. Remote Sens. Environ. 202, 18–27. https://doi.org/10.1016/j.rse.2017.06.031.

Hammer, Ø., Harper, D.A.T., Ryan, P.D., 2001. PAST: Paleontological statistics software package for education and data analysis. Palaeontol. Electron. 4, 9.

Holmes, R., 1983. Computer-assisted quality control in tree-ring dating and measurement. Tree Ring Bull. 43, 69–78.

Huang, M., Wang, X., Keenan, T.F., Piao, S., 2018. Drought timing influences the legacy of tree growth recovery. Glob. Chang. Biol. 24, 3546–3559. https://doi.org/10.1111/gcb.14294.

Huang, K., Xia, J., 2019. High ecosystem stability of evergreen broadleaf forests under severe droughts. Glob. Chang. Biol. 25, 3494–3503. https://doi.org/10.1111/gcb.14748.

Huete, A.R., Liu, H.Q., Batchily, K.V., Van Leeuwen, W.J., 1997. A comparison of vegetation indices over a global set of TM images for EOS-MODIS. Remote Sens. Environ. 59, 440–451. https://doi.org/10.1016/S0034-4257(96)00112-5.

Khoury, S., Coomes, D.A., 2020. Resilience of Spanish forests to recent droughts and climate change. Glob. Chang. Biol. 26, 7079–7098. https://doi.org/10.1111/gcb.15268.

Kiorapostolou, N., Petit, G., Dannoura, M., 2019. Similarities and differences in the balances between leaf, xylem and phloem structures in *Fraxinus ornus* along an environmental gradient. Tree Physiol. 39 (2), 234–242.

Lloret, F., Lobo, A., Estevan, H., Maisongrande, P., Vayreda, J., Terradas, J., 2007. Woody plant richness and NDVI response to drought events in Catalonian (Northeastern Spain) forests. Ecology 88, 2270–2279. https://doi.org/10.1890/06-1195.1.

Mašek, J., Tumajer, J., Lange, J., Kaczka, R., Fišer, P., Treml, V., 2023. Variability in tree-ring width and NDVI responses to climate at a landscape level. Ecosystems 26 (5), 1144–1157.

Matsushita, B., Yang, W., Chen, J., Onda, Y., Qiu, G., 2007. Sensitivity of the enhanced vegetation index (EVI) and normalized difference vegetation index (NDVI) to topographic effects: a case study in high-density cypress forest. Sensors 7, 2636–2651. https://doi.org/10.3390/s7112636.

Michelot, A., Simard, S., Rathgeber, C., Dufrêne, E., Damesin, C., 2012. Comparing the intra-annual wood formation of three European species (Fagus sylvatica, Quercus petraea and Pinus sylvestris) as related to leaf phenology and non-structural carbohydrate dynamics. Tree Physiol. 32, 1033–1043. https://doi.org/10.1093/treephys/tps052.

Moreno-Fernández, D., Camarero, J.J., García, M., Lines, E.R., Sánchez-Dávila, J., Tijerín, J., Valeriano, C., Viana-Soto, A., Zavala, M.Á., Ruiz-Benito, P., 2022. The Interplay of the Tree and Stand-Level Processes Mediate Drought-Induced Forest Dieback: Evidence from Complementary Remote Sensing and Tree-Ring Approaches. Ecosystems 25 (8), 1738–1753.

Ogaya, R., Barbeta, A., Basnou, C., Peñuelas, J., 2015. Satellite data as indicators of tree biomass growth and forest dieback in a Mediterranean holm oak forest. Ann. For. Sci. 72, 135–144. https://doi.org/10.1007/s13595-014-0408-y.

Poyatos, R., Llorens, P., Piñol, J., Rubio, C., 2008. Response of Scots pine (Pinus sylvestris L.) and pubescent oak (Quercus pubescens Willd.) to soil and atmospheric water deficits under Mediterranean mountain climateRéponses du pin sylvestre (Pinus sylvestris L.) et du chêne pubescent (Quercus pubescens Wild.) aux déficits hydriques atmosphérique et édaphique sous climat montagnard méditerranéen. Ann. For. Sci. 65 (3), 306.

Prendin, A.L., Carrer, M., Karami, M., Hollesen, J., Bjerregaard Pedersen, N., Pividori, M., Treier, U.A., Westergaard-Nielsen, A., Elberling, B.o., Normand, S., Zurell, D., 2020. Immediate and carry-over effects of insect outbreaks on vegetation growth in West Greenland assessed from cells to satellite. J. Biogeogr. 47 (1), 87–100.

Rita, A., Camarero, J.J., Nolè, A., Borghetti, M., Brunetti, M., Pergola, N., Serio, C., Vicente-Serrano, S.M., Tramutoli, V., Ripullone, F., 2020. The impact of drought spells on forests depends on site conditions: The case of 2017 summer heat wave in southern Europe. Glob. Chang. Biol. 26, 851–863. https://doi.org/10.1111/gcb.14825.

Rosner, S., 2012. Acoustic emission related to stomatal closure of four deciduous broad-leaved woody species. In 30th European Conference on Acoustic Emission Testing (EWGAE). EWGAE, Granada. J. Acoustic Emission, 30: 11-20.

Rouse, J., Haas, R., Schell, J., Deering, D., 1973. Monitoring Vegetation Systems in the Great Plains with ERTS. Third ERTS Symposium, NASA, pp. 309–317.

Schneider, C.A., Rasband, W.S., Eliceiri, K.W., 2012. NIH Image to ImageJ, 25 years of image analysis. Nat. Methods 9, 671–675. https://doi.org/10.1038/nmeth.2089.

Scholz, A., Klepsch, M., Karimi, Z., Jansen, S., 2013. How to quantify conduits in wood? Front. Plant Sci. 4, 1–11. https://doi.org/10.3389/fpls.2013.00056.

Schwarz, J., Skiadaresis, G., Kohler, M., Kunz, J., Schnabel, F., Vitali, V., Bauhus, J., 2020. Quantifying growth responses of trees to drought-a critique of commonly used resilience indices and recommendations for future studies. Curr. For. Rep. 6, 185–200. https://doi.org/10.1007/s40725-020-00119-2.

Sperry, J.S., Nichols, K.L., Sullivan, J.E.M., Eastlack, S.E., 1994. Xylem embolism in ring-porous, diffuse-porous, and coniferous trees of northern Utah and interior Alaska. Ecology 75, 1736–1752. https://doi.org/10.2307/1939633.

Sturm, J., Santos, M.J., Schmid, B., Damm, A., 2022. Satellite data reveal differential responses of Swiss forests to unprecedented 2018 drought. Glob. Chang. Biol. 28, 2956–2978. https://doi.org/10.1111/gcb.16136.

Tognetti, R., Longobucco, A., Raschi, A., 1999. Seasonal embolism and xylem vulnerability in deciduous and evergreen Mediterranean trees influenced by proximity to a carbon dioxide spring. Tree Physiol. 19 (4–5), 271–277. https://doi.org/10.1093/treephys/19.4-5.271.

Tomasella, M., Casolo, V., Aichner, N., Petruzzellis, F., Savi, T., Trifilò, P., Nardini, A., 2019. Non-structural carbohydrate and hydraulic dynamics during drought and recovery in Fraxinus ornus and Ostrya carpinifolia saplings. Plant Physiol. Biochem. 145, 1–9. https://doi.org/10.1016/j.plaphy.2019.10.024.

Tonelli, E., Vitali, A., Malandra, F., Camarero, J.J., Colangelo, M., Nolè, A., Ripullone, F., Carrer, M., Urbinati, C., 2023. Tree-ring and remote sensing analyses uncover the role played by elevation on European beech sensitivity to late spring frost. Sci. Total Environ. 857, 159239.

Tyree, M.T., Zimmermann, M.H., 2002. Xylem structure and the ascent of sap. Springer, Berlin, Germany.

Vicente-Serrano, S.M., Beguería, S., López-Moreno, J.I., 2010. A multiscalar drought index sensitive to global warming: The Standardized Precipitation Evapotranspiration Index. J. Clim. 23, 1696–1718. https://doi.org/10.1175/2009JCLI2909.1.

Vicente-Serrano, S.M., Gouveia, C., Camarero, J.J., Beguería, S., Trigo, R., López-Moreno, J.I., Azorín-Molina, C., Pasho, E., Lorenzo-Lacruz, J., Revuelto, J., Morán-Tejeda, E., Sanchez-Lorenzo, A., 2013. Response of vegetation to drought time-scales across global land biomes. PNAS 110 (1), 52–57.

Vicente-Serrano, S.M., Martín-Hernández, N., Camarero, J.J., Gazol, A., Sánchez-Salguero, R., Peña-Gallardo, M., El Kenawy, A., Domínguez-Castro, F., Tomas-Burguera, M., Gutiérrez, E., de Luis, M., Sangüesa-Barreda, G., Novak, K., Rozas, V., Tíscar, P.A., Linares, J.C., del Castillo, E.M., Ribas, M., García-González, I., Silla, F., Camisón, A., Génova, M., Olano, J.M., Longares, L.A., Hevia, A., Diego Galván, J., 2020. Linking tree-ring growth and satellite-derived gross primary growth in multiple forest biomes. Temporal-scale matters. Ecol. Indic. 108, 105753.

Wang, Z., Lyu, L., Liu, L., Liang, H., Huang, J., Zhang, Q.B., 2021. Topographic patterns of forest decline as detected from tree rings and NDVI. Catena 198, 105011. https://doi.org/10.1016/j.catena.2020.105011.